Spectrum of second-harmonic generation for multimode fields

Y. B. Band
Ben-Gurion University, Beer Sheva, 84105 Israel

D. F. Heller
Light Age, Inc., 6 Powderhorn Drive, Mt. Bethel, New Jersey 07060

J. R. Ackerhalt
Los Alamos National Laboratory, Los Alamos, New Mexico 87545

J. S. Krasinski
Allied-Signal Inc., Corporate Technology Center, Morristown, New Jersey 07960
(Received 5 February 1990)

We calculate the spectrum of second-harmonic generation (SHG) for multimode input fields. We show that SHG *cannot* be described as the degenerate limit of sum-frequency generation (SFG) for multimode fields, because the dynamical equations describing SFG do not properly account for this degeneracy. We consider SHG for amplitude-modulated as well as frequency-modulated fundamental fields. The bandwidth of the second harmonic generated from an amplitude-modulated fundamental field depends on the fundamental input intensity and the conversion strength of the nonlinear medium. Additional frequencies that are not contained in the set of frequencies $\omega_{1i}+\omega_{1j}$ will be created at intermediate conversion strengths. However, the growth of the spectral bandwidth is much less pronounced than in SFG. For very high conversion, the spectrum of the second harmonic narrows with increased conversion strength. For frequency-modulated input fields, the second-harmonic spectrum is independent of both the fundamental input intensity and the conversion strength.

I. INTRODUCTION

The theory of three-wave mixing for single-mode fields was formulated in a classic paper by Armstrong *et al.* over 25 years ago.[1] Modern descriptions of these processes [sum-frequency generation (SFG), difference-frequency generation (DFG), second-harmonic generation (SHG), parametric oscillation (PO)] are available in many textbooks on nonlinear optics and quantum electronics[2–4] and are essentially identical to that of the original article. Recently, a theoretical description of three-wave mixing for multimode time-dependent input fields (as opposed to cw single-frequency time-independent input fields) was presented,[5] and analytic solutions were developed for the time-dependent intenseties of the output fields. These solutions differ dramatically from those for single-mode fields. New frequencies in the sum-frequency output spectrum and in the input-field output spectrum are created and grow in magnitude as the input intensities are increased. The output spectrum broadens under conditions of strong nonlinear coupling, ultimately reaching the phase-matched bandwidth limit.

Reference 5 deals with SFG of multimode input fields. In this paper, we shall explicitly consider second-harmonic generation. We shall show that SHG cannot be described as a limit of the SFG formalism for multimode fields. The SFG formulation for the interaction of photons close to frequency ω_1 with photons close to frequency ω_2 producing photons close to frequency $\omega_3=\omega_1+\omega_2$ does not allow ω_1 (ω_2) photons to interact with each other to produce photons close to frequency $2\omega_1$ ($2\omega_2$). This self-interaction is crucial for SHG and must be incorporated. Therefore, a separate formulation is used to describe SHG with multimode input fields. Figure 1 schematizes the frequencies obtained in SFG and SHG to lowest order in the weak conversion limit. The different interactions considered in SFG and SHG are explicitly shown. Specifically, the SFG formalism treats only the mixing of fields with central frequency ω_1 and ω_2, i.e., those processes that are assumed to be phase matched, as described in the bottom of Fig. 1, and does not allow for generation of frequencies outside the phase-matched bandwidth region shown in the bottom of the figure. It should be stressed, however, that the output spectra for both SHG and SFG can be much wider than the lowest-order perturbation theory scheme shown in the figure.

We shall calculate the spectrum of SHG for multimode input fields. One important quantity associated with the spectrum is its bandwidth. In previous studies, many authors have considered the bandwidth of SHG and have assumed that the bandwidth of the output is twice the bandwidth of the fundamental. This estimate was based upon the bandwidth as obtained in the perturbation-theory limit as shown in Fig. 1. However, as we shall see, the bandwidth depends on the intensity of the input and the conversion strength of the nonlinear medium. Additional frequencies that are not contained in the set of frequencies $\omega_{1i}+\omega_{1j}$, where ω_{1i} are the cavity mode fre-

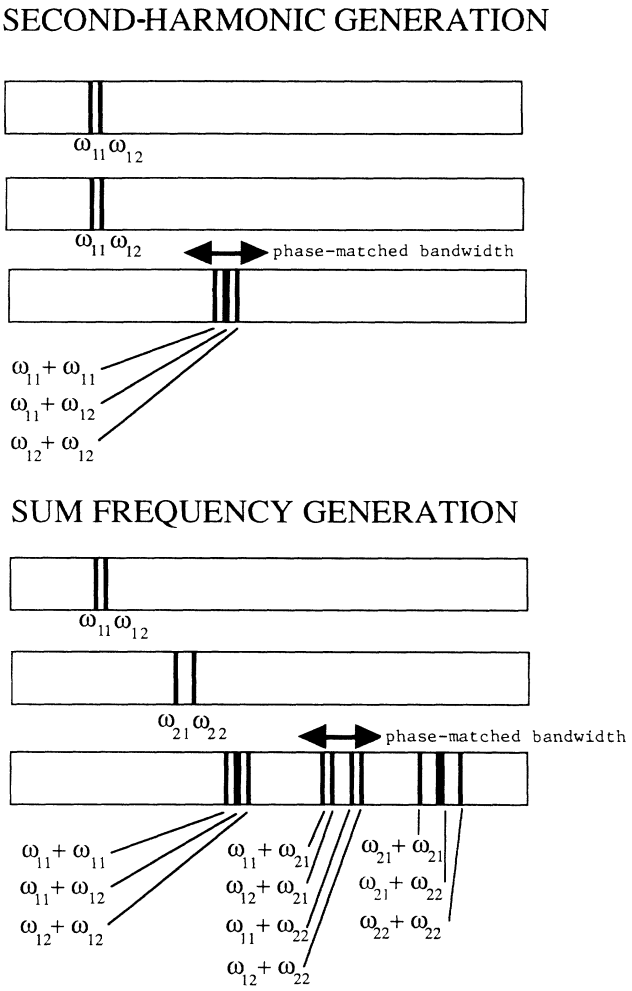

FIG. 1. Schematic of the frequencies obtained in SFG and SHG to lowest order in the weak conversion limit. The different interactions considered in SFG and SHG are explicitly described. The SFG formalism assumes that only the processes occurring in the phase-matched frequency region occur.

quencies of the fundamental laser, $\omega_{1j}\equiv\omega_1+\Delta j$, and Δ is the mode frequency spacing of the laser cavity, are created at sufficiently high conservation strengths as depletion of the fundamental occurs. However, the growth of the bandwidth with increasing input intensity of the fundamental and with increasing nonlinear coupling strength is very much reduced compared with the SFG case. Moreover, at the highest conservation strengths the spectrum of the second harmonic actually shrinks.

We shall study SHG for both amplitude- and frequency-modulated fields. In Ref. 5 we studied SFG for amplitude-modulated time-dependent input fields because an analytic solution exists in that case. This is also true for SHG, but no analytic solution is known for the frequency-modulated case. Therefore, we have found using numerical integration that for the frequency-modulated case, the second-harmonic spectrum is independent of both the fundamental input intensity and the conversion strength.

There are interesting differences in the nature of the spectrum of SHG and SFG. For example, consider SHG with an input field consisting of three modes of equal amplitude at frequencies ω_{11}, $\omega_{12}=\omega_{11}+\Delta$, and $\omega_{13}=\omega_{11}-\Delta$. The output spectrum consists of a discrete nondense spectrum with frequencies $2\omega_{11}+m\Delta$, where m is an integer, with $m=0,\pm1,\pm2$ being the largest amplitude components. For SFG with input fields each containing three modes, ω_{11} (ω_{21}), $\omega_{12}=\omega_{11}+\Delta_1$ $(\omega_{22}=\omega_{21}+\Delta_2)$, and $\omega_{13}=\omega_{11}-\Delta_1$ $(\omega_{23}=\omega_{21}-\Delta_2)$ in the first (second) field, the output spectrum can be dense if Δ_1 and Δ_2 are incommensurate (i.e., Δ_1/Δ_2 is not rational) and will consist of components at frequencies $\omega_{11}+\omega_{21}+m\Delta_2+n\Delta_1$, where m and n are all positive and negative integers. Thus the nature of the spectra can be completely different. As we shall see, many other differences also exist.

In Sec. II we describe the differences in the formulations for SHG and SFG and discuss the reasons for these differences. In Sec. III we calculate the spectrum of SHG for multimode input fields in the weak, intermediate, and strong conversion regimes for amplitude- and frequency-modulated input fields, and compare these results with SFG. Section IV contains a conclusion and summary.

II. DIFFERENCES OF SHG AND SFG FORMALISMS

The dynamical equations governing SFG of phase-matched plane waves are given in the slowly varying envelope approximation by[5]

$$\begin{aligned}\frac{\partial E_1(z,\tau)}{\partial z}&=-i\omega_1\chi E_3E_2^*\ ,\\ \frac{\partial E_2(z,\tau)}{\partial z}&=-i\omega_2\chi E_3E_1^*\ ,\\ \frac{\partial E_3(z,\tau)}{\partial z}&=-i\omega_3\chi E_1E_2\ ,\end{aligned}\tag{1}$$

where E_1, E_2, and E_3 are the complex interacting electric-field envelopes, ω_1, ω_2, and ω_3 are their frequencies, τ is the local pulse time $(\tau=t-z/c)$, z is the distance in the medium, and χ is the nonlinear polarization coefficient for three-wave mixing. Analytic solutions for the intensities, defined here as the absolute square of the electric fields, for real χ and real input fields are

$$I_3(z,\tau)=\frac{\omega_3}{\omega_{\min}}I_{\min}(0,\tau)\,\mathrm{sn}^2\left[[I_{\max}(0,\tau)]^{1/2}\omega_{\max}\chi z,\left[\frac{\omega_{\max}I_{\min}(0,\tau)}{\omega_{\min}I_{\max}(0,\tau)}\right]^{1/2}\right],$$
$$I_1(z,\tau)=I_1(0,\tau)-\frac{\omega_1}{\omega_3}I_3(z,\tau),\quad I_2(z,\tau)=I_2(0,\tau)-\frac{\omega_2}{\omega_3}I_3(z,\tau)\ .\tag{2}$$

Here sn(.,.) is the doubly periodic Jacobi elliptic function,[6] $E_i(0,\tau)$ and $I_i(0,\tau)$ are the electric field and the intensity incident, respectively, upon the sample at time τ, $I_{\min}(0,\tau)$ [$I_{\max}(0,\tau)$] is the smaller [larger] of the input fields $I_1(0,\tau)$ and $I_2(0,\tau)$. These solutions are appropriate even when fields 1 and 2 are multifrequency beams. The Manley-Rowe relationship,

$$\frac{\partial}{\partial z}[I_1(z,\tau)/\omega_1+I_2(z,\tau)/\omega_2+2I_3(z,\tau)/\omega_3]=0 , \tag{3}$$

ensures conservation of photon numbers ($N_i=I_i/c\hbar\omega_i$) and is a direct consequence of Eqs. (1).

The plane-wave equations governing SHG if we assume phase matching are given in the slowly varying envelope approximation by

$$\begin{aligned}\frac{\partial E_1(z,\tau)}{\partial z}&=i\omega_1\chi E_3 E_1^* ,\\ \frac{\partial E_3(z,\tau)}{\partial z}&=-i\omega_1\chi E_1^2 .\end{aligned} \tag{4}$$

Analytic solutions for the electric fields for real χ and real input field envelope $E_1(0,\tau)$ are

$$\begin{aligned}E_3(z,\tau)&=-iE_1(0,\tau)\tanh[E_1(0,\tau)\omega_1\chi z] ,\\ E_1(z,\tau)&=E_1(0,\tau)\operatorname{sech}[E_1(0,\tau)\omega_1\chi z] ,\end{aligned} \tag{5}$$

and therefore intensities are

$$\begin{aligned}I_3(z,\tau)&=I_1(0,\tau)\tanh^2[\sqrt{I_1(0,\tau)}\omega_1\chi z] ,\\ I_1(z,\tau)&=I_1(0,\tau)\operatorname{sech}^2[\sqrt{I_1(0,\tau)}\omega_1\chi z] .\end{aligned} \tag{6}$$

These solutions are appropriate even when the fundamental field has multifrequency components, as long as the input field is real and provided the fundamental field remains within the phase-matching bandwidth throughout the propagation in the crystal. When the envelope $E_1(0,\tau)$ is not real, Eqs. (4) must be numerically solved.

Equation (4) for SHG *cannot* be obtained as a limiting case of Eqs. (1) for SFG when $\omega_1=\omega_2=\omega_3/2$ and $E_1=E_2$. A straightforward calculation using these relationships in Eqs. (1) gives

$$\begin{aligned}\frac{\partial E_1(z,\tau)}{\partial z}&=-i\omega_1\chi E_3 E_1^* ,\\ \frac{\partial E_3(z,\tau)}{\partial z}&=-i2\omega_1\chi E_1^2 ,\end{aligned} \tag{7}$$

which obviously disagrees with Eq. (4) by a factor of 2 in the frequency in the second equation. The reason for this surprising result is that in the SFG formalism as it is presently derived which describes production of an ω_3 photon from one ω_1 photon and one ω_2 photon, the frequencies ω_1 and ω_2 are required to be nondegenerate. For SHG this degeneracy is not only allowed, but is the essence of the process. Thus the SFG formalism in reality is not compatible with the SHG process. A complete formalism encompassing both phenomena simultaneously is possible, but will not be developed here.

It is easy to verify that the Manley-Rowe relationship obtained from Eqs. (4),

$$\frac{\partial}{\partial z}[I_1(z,\tau)/\omega_1+2I_3(z,\tau)/\omega_3]=0 , \tag{8}$$

correctly describes SHG, since for every two photons converted from field I_1, we obtain one photon from field I_3. Obviously the Manley-Rowe condition that one obtains from Eq. (7) or, equivalently, from Eq. (3) with $\omega_1=\omega_2$ and $I_1=I_2$ is incorrect in that it predices a one-to-one photon conversion.

When the slowly varying envelope of the input field is not purely real, the phase of the envelope plays a role in the dynamics. This is evident by rewritting Eq. (4) in terms of the amplitudes and phases of the envelopes, $E_1(z,\tau)=A_1(z,\tau)\exp[i\theta_1(z,\tau)]$ and $E_3(z,\tau)=-iA_3(z,\tau)\exp[i\theta_3(z,\tau)]$. Equation (4) then becomes

$$\begin{aligned}\frac{\partial A_1(x,\tau)}{\partial z}&=-\omega_1\chi A_3 A_1\cos(\theta_3-2\theta_1) ,\\ \frac{\partial A_3(z,\tau)}{\partial z}&=\omega_1\chi A_1^2\cos(\theta_3-2\theta_1) ,\\ \frac{\partial\theta_1(z,\tau)}{\partial z}&=-\omega_1\chi A_3\sin(\theta_3-2\theta_1) ,\\ \frac{\partial\theta_3(z,\tau)}{\partial z}&=-\omega_1\chi A_1^2/A_3\sin(\theta_3-2\theta_1) .\end{aligned} \tag{9}$$

Thus the phases of the electric-field envelopes dynamical evolve only if $\sin(\theta_3-2\theta_1)$ is initially nonzero, which is trivially satisfied for $\theta_3=\theta_1=0$.

III. SPECTRUM OF MULTIMODE SHG

We shall now present the spectra of the second-harmonic output and the fundamental output upon SHG of a multimode fundamental field in the weak, intermediate, and strong conversion regimes. We consider the case where the fundamental field originates from a laser emitting light at several cavity mode frequencies. The temporal dependence of the input electric field, $F_1(0,\tau)$, can then be written as

$$\begin{aligned}F_1(0,\tau)&=\exp(i\omega_1\tau)E_1(0,\tau)+\text{c.c.}\\ &=\exp(i\omega_1\tau)\sum_{j=-n}^{n}E_{1,j}\exp[i(\Delta j\tau+\phi_{1,j})]=\text{c.c.} ,\end{aligned} \tag{10}$$

where we can define the cavity mode frequencies as $\omega_{1,j}\equiv\omega_1+\Delta j$, Δ is the mode frequency spacing of the cavity, and $\phi_{1,j}$ are the phase shifts for the different mode. The SHG solution, Eq. (5) is valid provided that the spectrum of the fundamental field is entirely within the phase-matching bandwidth of the crystal. As we shall see, the output spectrum can be much wider than the set of frequencies $\omega_{3,j,j'}=\omega_{1,j}+\omega_{1,j'}=2\omega_1+\Delta(j+j')$, where $j,j'=-n,n$.

We define the (dimensionless) coupling strength parameter u as $u\equiv\{\sup_\tau[I_1(\tau)]\}^{1/2}\omega_1\chi L$, where L is the length of nonlinear crystal through which the light propagates. Note that u is the maximum argument of the hyperbolic functions in the analytic solutions, Eqs. (5) and (6). In

what follows, we designate very low, low, medium, and high coupling strengths as follows: $u=5\times10^{-3}$, 5×10^{-2}, 0.5, and 5, respectively.

We first consider the case of SHG when the input beam contains three equal intensity modes, i.e., $n=1$ in Eq. (3), with $E_{1,-1}=E_{1,0}=E_{1,1}=\frac{1}{3}$, and $\phi_{1,-1}=\phi_{1,0}=\phi_{1,1}=0$. The slowly varying envelope is given by $E_1(0,\tau)=[1+2\cos(\Delta\tau)/3]$. This field is amplitude modulated and is similar to the fields considered in Ref. 5 in the studies of SFG. For comparison, we shall also consider the case of an amplitude-modulated field with seven modes but identical values of u, $E_1(0,\tau)=[1+2\cos(\Delta\tau)+2\cos(2\Delta\tau)+2\cos(3\Delta\tau)]/7$.

Figures 2 and 3 show the temporal dependence of the fundamental and SHG output at frequencies around ω_1 and $\omega_3=2\omega_1$, respectively, for the three-mode input case. The output after propagation through a nonlinear mixing crystal, is plotted in these figures for input fields with very low, medium, and high coupling strengths. The temporal dependence is periodic, with one period shown in the figures. The intensity at ω_3 reflects the fact that $I_1(\tau)$ must be large for $I_3(\tau)$ to be large; in the very low conversion limit, $I_3(L,\tau)\propto[I_1(0,\tau)]^2$. Depletion of the input is clear in the medium and high coupling strength cases. At very low coupling strengths, almost none of the fundamental is converted, and therefore the input fundamental intensity is almost identical to the output fundamental intensity, and a separate figure showing the input field is not necessary.

Figures 4 and 5 are similar to Figs. 2 and 3, respectively, except for the seven-mode input case. For high coupling strengths, almost all the fundamental is converted into the second harmonic, such that the intensity profile of the second harmonic looks like the input fundamental for both the three- and seven-mode input field cases. Only about 1% remains in the fundamental for the high coupling strength cases.

In the study of SFG, sharp temporal features originate from reconversion of $I_3(\tau)$ back into $I_1(\tau)$ and $I_2(\tau)$, and vice versa. When the weaker of $I_1(\tau)$ and $I_2(\tau)$ is fully depleted, $I_3(\tau)$ and the remaining intensity mix and reform the weaker input field. This property can be understood in terms of the analytic solution to the SFG dynamics, which involves the double periodic Jacobi elliptic function, $\mathrm{sn}(x(\tau),y(\tau))$. The first argument of the an(.,.) function is proportional to the magnitude of the larger of

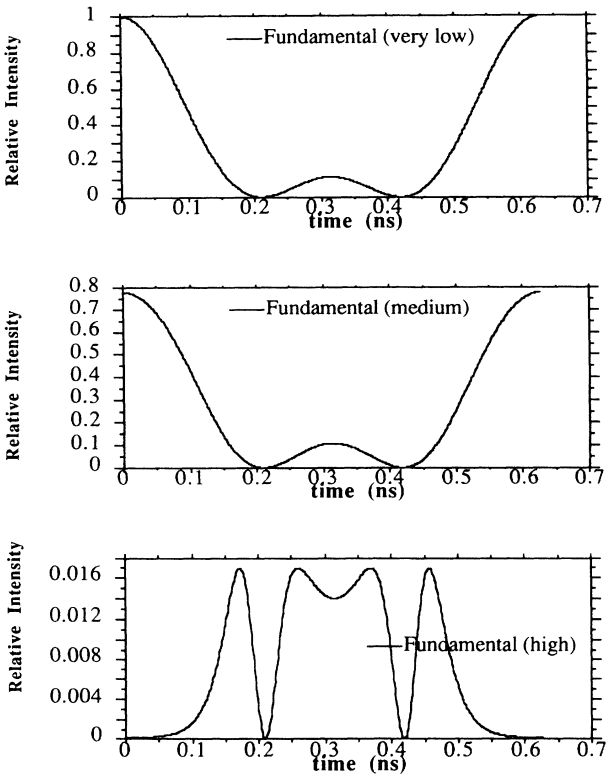

FIG. 2. Temporal dependence of the fundamental output at frequencies around ω_1 for an input fundamental field with three modes. The output after propagation through a nonlinear mixing crystal is plotted in these figures for input fields with very low, medium, and high coupling strengths, corresponding to $u=5\times10^{-3}$, 0.5, and 5, respectively. In the very low frequency case, the input pulse is virtually identical to the output pulse, and so there is no need for a separate figure of the input pulse shape. The temporal dependence of the field is periodic and recurs outside the period plotted in the figure.

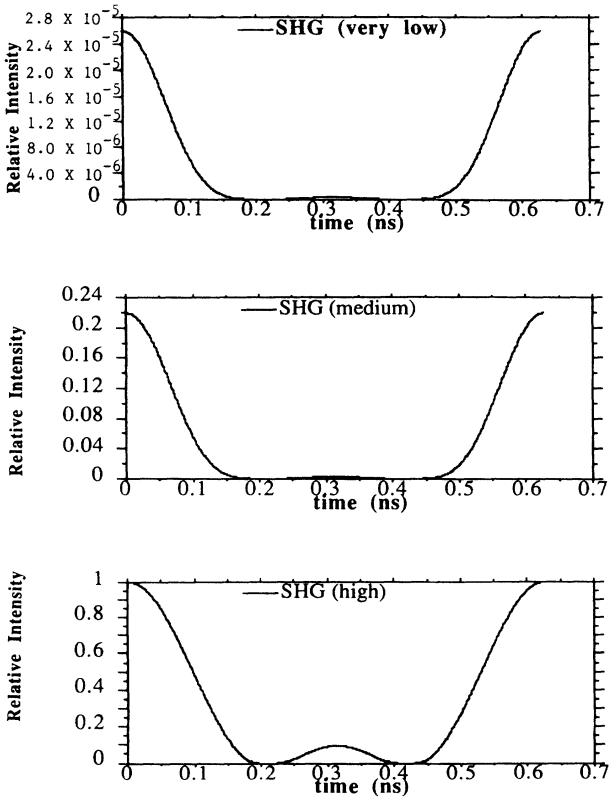

FIG. 3. Temporal dependence of the second-harmonic output at frequencies around $2\omega_1$ for the input fundamental field with three modes shown in Fig. 2. The output after propagation through a nonlinear mixing crystal is plotted in these figures for input fields with very low, medium, and high coupling strengths, corresponding to $u=5\times10^{-3}$, 0.5, and 5, respectively.

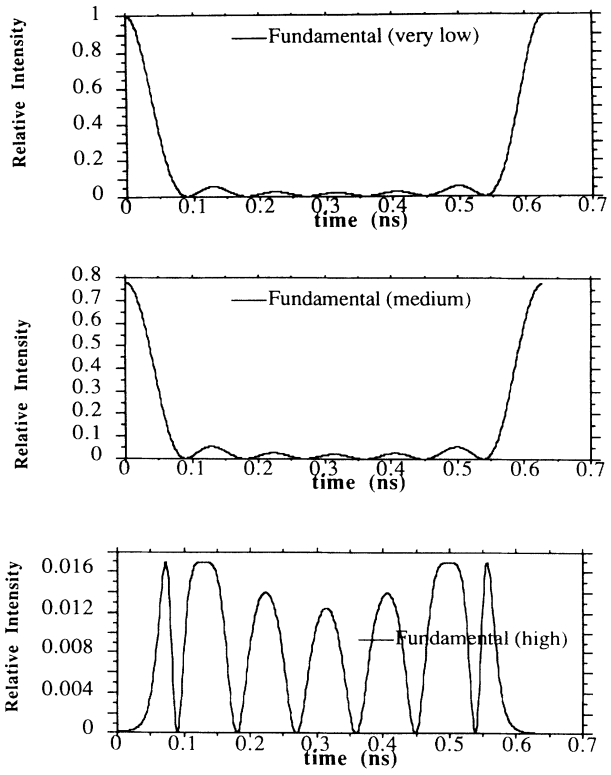

FIG. 4. Same as Fig. 2, except for an input fundamental field with seven modes.

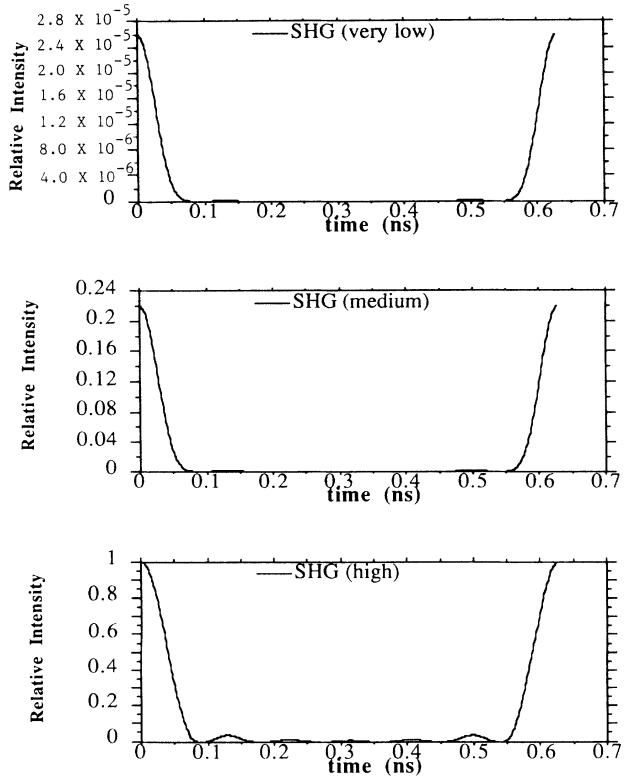

FIG. 5. Same as Fig. 3, except for an input fundamental field with seven modes.

the input fields, and the second argument is proportional to the ratio of the smaller and the larger input fields.[5] When the first argument is large and varies with time, spiky features in the temporal dynamics result. These features do not occur for SHG, as is evident from Figs. 1–4. In SHG, when $I_1(\tau)$ is depleted, no reconversion can occur. The analytic solution for SHG, $\tanh(x)$, is monotonic with x, whereas the doubly periodic Jacobi elliptic function, $\mathrm{sn}(x,y)$, is periodic with x, except for $y=1$, where $\mathrm{sn}(x,1)=\tanh(x)$. The intensity of SFG is proportional to $y\,\mathrm{sn}^2(x,y)$. In Fig. 6, we plot $y\,\mathrm{sn}^2(x,y)$ vs x for several values of y. As $x(\tau)$ varies with τ, $y(\tau)\mathrm{sn}^2(x(\tau),y(\tau))$ wildly fluctuates, unless $y(\tau)=1$, as is the case for SHG. Therefore, the Fourier transform is the SHG field contains fewer frequency components than in the SFG case.

Figure 7 shows the Fourier transform of the output field near frequency ω_3 at different coupling strengths for the three-mode input case. Note that the absolute value square of the Fourier transform of the slowly varying envelope of the output field $|E_3(L,2\omega+j\Delta)|^2$ is plotted. Figure 8 is similar to Fig. 7, except it is for the seven-mode input case. Zero frequency in Figs. 7 and 8 corresponds to the output at frequency $2\omega_1$, and frequency j corresponds to output at frequencies $2\omega_1+j\Delta$. In Fig. 7, the largest components in the spectrum are at -2Δ, $-\Delta$, 0, Δ, and 2Δ, as is to be expected, but even at very low coupling strengths other components are present. Additional frequency components become more significant at low and medium coupling strengths. However, at very high coupling strengths, these additional frequency components become much weaker, and even the

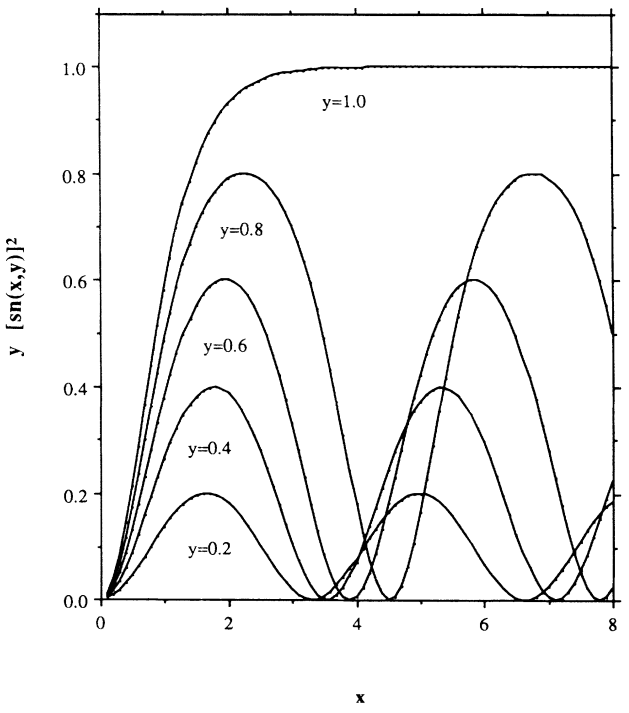

FIG. 6. $\mathrm{sn}^2(x,y)$ vs x for several values of y.

components at -2Δ and 2Δ decrease substantially! This is due to the fact that the second harmonic takes on the temporal shape of the fundamental at very high conversion, and the fundamental only contains the components $-\Delta$, 0, and Δ for the three-mode case. From the simple analysis described in Fig. 1, we expect the ratio of the frequency components of the intensities $|E_3(L,2\omega+\Delta)|^2/|E_3(L,2\omega)|^2$ and $|E_3(L,2\omega+2\Delta)|^2/|E_3(L,2\omega)|^2$ to be $(\frac{2}{3})^2(\approx 0.444)$ and $(\frac{1}{3})^2(\approx 0.111)$, respectively. This is because there are three ways of forming frequency 2ω, two ways of forming frequency $2\omega+\Delta$, and only one way of forming frequency $2\omega+2\Delta$. The actual ratios obtained in the three-mode case are very close to these values for the very low conversion strength case. The ratio $|E_3(L,2\omega+3\Delta)|^2/|E_3(L,2\omega)|^2$ is calculated to be 0.013 for the very low conversion strength case, whereas perturbation theory yields zero. Similar behavior occurs for the seven-mode input case.

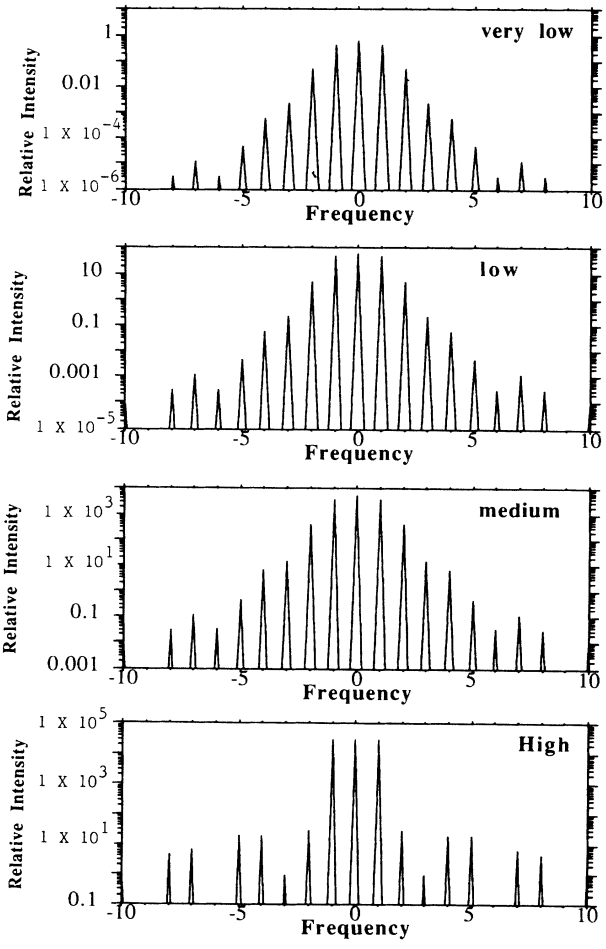

FIG. 7. Fourier transform of the output field near frequency ω_3, $|E_3(L,2\omega+j\Delta)|^2$, at different coupling strengths for an input field with three modes. Zero frequency corresponds to output at frequency $2\omega_1$, and frequency j corresponds to output at frequencies $2\omega_1+j\Delta$, i.e., the frequency scale is in units of Δ. The output designated very low, low, medium, and high coupling strengths correspond to $u=5\times10^{-3}$, 5×10^{-2}, 0.5, and 5, respectively.

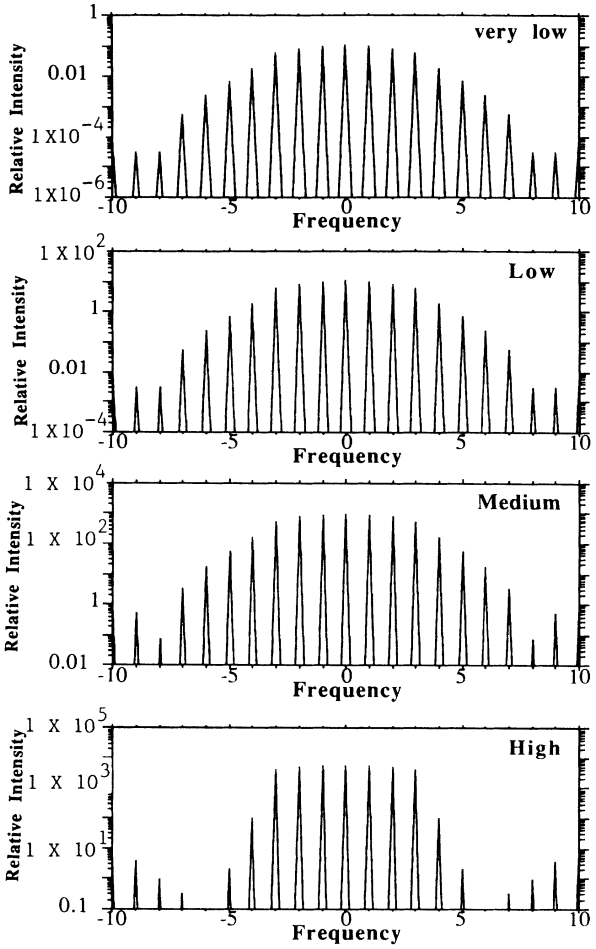

FIG. 8. Same as Fig. 7, except the input field has seven modes.

IV. FREQUENCY-MODULATED FUNCTIONAL FIELDS

We now consider the case of an input field which is frequency modulated. An analytic solution for this case is not available, so we integrate Eqs. (4) from $z=0$ to L. We take $L=1$ cm and choose $\omega_1\chi$ such that u takes on the values of $u=5\times10^{-3}$, 5×10^{-2}, 0.5, and 5, respectively. We consider a frequency-modulated field of the form $E_1(0,\tau)=\exp[i\cos(\Delta\tau)5\Delta\tau]$. The output is constant with time and with second-harmonic output intensities of the very low, low, medium, and high cases given by 2.58×10^{-5}, 2.58×10^{-3}, 0.220 and 0.9998, respectively. Even though the intensity is temporally constant, there are multiple frequencies contained in the spectrum. Figure 9 shows the Fourier transform of the output field around central frequency $\omega_3=2\omega_1$ for different coupling strengths. Amazingly, there is no change in the spectrum with coupling strength. The magnitude of the second-harmonic frequency components naturally changes with increased coupling strength, but the ratio of the amplitudes of the different frequency components remains unchanged. Thus, the spectral content for second-harmonic generation is independent of both the fundamental input intensity and the coupling strength for frequency-modulated input fields.

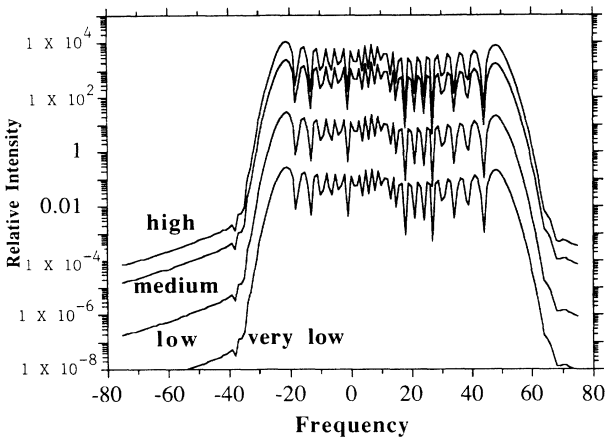

FIG. 9. Same as Fig. 7, except the input field is frequency modulated.

V. SUMMARY AND CONCLUSION

We showed that SHG cannot be described as a limit of the SFG formalism. In SHG, the interaction of a photon with another photon of the same frequency is crucial and must be incorporated, but the SFG formalism does not allow for this type of interaction. Therefore, a separate formalism is necessary to describe SHG with multimode input fields. We discussed the similarities and differences in the nature of the spectrum of SHG and SFG. We used the analytic and numerical solutions for the dynamical equations describing SHG to study the generated spectrum. We considered SHG for amplitude-modulated as well as frequency-modulated input fields. We showed that the spectrum of the second harmonic depends on the intensity of the fundamental input and the conversion strength of the nonlinear medium for amplitude-modulated input fields. However, the growth of the bandwidth with increased fundamental input intensity and the conversion strength of the nonlinear medium is much less pronounced than in SFG. In the very high coupling strength case, almost all the fundamental is converted into second harmonic. Therefore the temporal dependence of the intensity of the second harmonic looks like that of the fundamental input intensity, and the spectrum of the second harmonic actually narrows relative to the lower coupling strength cases. In addition, we found that the spectrum for frequency-modulated input fields is independent of both the intensity of the fundamental input and the coupling strength.

ACKNOWLEDGMENTS

This work was partially supported by a grant from the U.S.-Israel Binational Science Foundation.

[1] J. A. Armstrong, N. Bloembergen, J. Ducuing, and P. S. Pershan, Phys. Rev. **127**, 1918 (1962).

[2] N. Bloembergen, *Nonlinear Optics* (Benjamin, New York, 1965).

[3] Y. R. Shen, *The Principles of Nonlinear Optics* (Wiley, New York, 1984), pp. 67–140.

[4] A. Yariv, *Quantum Electronics*, 3rd ed. (Wiley, New York, 1975).

[5] Y. B. Band, D. F. Heller, and J. S. Krasinski, Phys. Rev. A **40**, 4400 (1989). A typographical error in the second argument of the sn function in Eq. (2) of this reference is corrected here in Eq. (2). The slowly varying envelopes of the input fields in this reference had three frequency components, ω_1, $\omega_1+\Delta_1$, and $\omega_1-\Delta_1$, with relative strengths 1, $\frac{1}{2}$, and $\frac{1}{2}$, respectively, and ω_2, $\omega_2+\Delta_2$, and $\omega_2-\Delta_2$, with relative strengths 1, $\frac{1}{2}$, and $\frac{1}{2}$, respectively. This may not have been clear from the disscussion in the reference. The SFG spectrum expected from perturbation theory are the five frequencies $\omega_1+\omega_2$, $\omega_1+\omega_2+\Delta_1-\Delta_2$, $\omega_1+\omega_2+\Delta_1$, $\omega_1+\omega_2+\Delta_2$, and $\omega_1+\omega_2+\Delta_1+\Delta_2$, as shown in Figs. 4 and 6 of that paper, together with the four frequency components symmetrically displaced about $\omega_1+\omega_2$ at $\omega_1+\omega_2-(\Delta_1-\Delta_2)$, $\omega_1+\omega_2-\Delta_1$, $\omega_1+\omega_2-\Delta_2$, and $\omega_1+\omega_2-(\Delta_1+\Delta_2)$, which were not plotted in Figs. 4 and 6 since they have the same strength as their symmetrically displaced counterparts (zero frequency in Figs. 4 and 6 corresponds to frequency $\omega_1+\omega_2$). Here we have chosen to plot the absolute value square of the Fourier transform of the slowly varying envelope of the sum-frequency output field, $|E_3(L,2\omega+j\Delta)|^2$, for positive as well as negative j, not the power spectrum for positive j plotted in Figs. 4 and 6 of this reference.

[6] *Handbook of Mathematical Functions*, Natl. Bur. Stand. Appl. Math. Ser. No. 55, edited by M. Abramowitz and I. Stegun (U.S. GPO, Washington, D.C., 1964), pp. 569–581.